Atmospheric ozone and colors of the Antarctic twilight sky

Raymond L. Lee, Jr.,[1,*] Wolfgang Meyer,[2] and Götz Hoeppe[3]

[1]Mathematics and Science Division, United States Naval Academy, Annapolis, Maryland 21402, USA

[2]Berufsgenossenschaftliche Unfallklinik Duisburg, Grossenbaumer Allee 250, 47247 Duisburg, Germany

[3]Department of Anthropology, College of William and Mary, Williamsburg, Virginia 23187, USA

*Corresponding author: raylee@usna.edu

Received 25 May 2011; revised 16 August 2011; accepted 19 August 2011;
posted 12 September 2011 (Doc. ID 147913); published 30 September 2011

Zenith skylight is often distinctly blue during clear civil twilights, and much of this color is due to preferential absorption at longer wavelengths by ozone's Chappuis bands. Because stratospheric ozone is greatly depleted in the austral spring, such decreases could plausibly make Antarctic twilight colors less blue then, including at the zenith. So for several months in 2005, we took digital images of twilight zenith and antisolar skies at Antarctica's Georg von Neumayer Station. Our colorimetric analysis of these images shows only weak correlations between ozone concentration and twilight colors. We also used a spectroradiometer at a midlatitude site to measure zenith twilight spectra and colors. At both locations, spectral extinction by aerosols seems as important as ozone absorption in explaining colors seen throughout the twilight sky. © 2011 Optical Society of America

OCIS codes: 010.1030, 010.1290, 010.1690, 010.3920, 010.4950, 330.1730.

1. Introduction

Hulburt's 1953 paper on sky colors [1] provided the first satisfactory explanation of the blues seen in the clear twilight sky: near the zenith, they are largely caused by ozone absorption rather than by molecular scattering. Hulburt's calculations show that spectral absorption by ozone's Chappuis bands accounts for much of the blue observed during twilight, a period when Rayleigh's scattering spectrum is far less important. The radiative balance shifts during twilight because ozone absorption (1) increases rapidly with increasing slant-path optical thickness through the stratosphere's ozone and (2) preferentially removes photons that contribute to the yellow and orange in direct sunlight. That the atmosphere's vanishingly small concentration of ozone could predominate in transforming sunlight into twilight's often vivid blues was a remarkable, but not unprecedented, insight. As Hulburt himself notes, Dubois' skylight measurements during twilight had already identified ozone absorption as being responsible for the unusual blue of the Earth's shadow (or dark segment) [2].

Ozone research soon became a staple in the optics of twilight, producing a steady trickle of works that detailed advances in both the measurement and modeling of its colors [3–5]. Gadsden's paper is particularly noteworthy because it seems to be the first that compares twilight's observed chromaticity coordinates (measured using a portable colorimeter) with those predicted by radiative calculations [6]. In his landmark book *Twilight*, Rozenberg [7] proposed an elaborate single-scattering model for a molecular atmosphere in which skylight spectra depend on what he calls the "effective height of the earth's shadow," itself a function of viewing direction and solar elevation. This alone, he argues, is sufficient to create a realistic gamut of sky colors during twilight, a gamut that presumably includes a bluish zenith. Rozenberg analyzes color with a low-resolution technique that Volz also uses: calculating the color ratios of skylight intensities in two narrow spectral bands [8].

0003-6935/11/28F162-10$15.00/0

Dave and Mateer [9] improved upon both Rozenberg's twilight model and its color analysis by (1) adding vertical profiles of ozone and dust and (2) calculating CIE chromaticity curves that result from scanning along sky meridians. Their conclusions about ozone agree with those of Hulburt and Gadsden, namely, that the twilight zenith in a purely molecular atmosphere without ozone can be slightly yellowish but never blue. Dave and Mateer add varying amounts of ozone to their single-scattering model, which restores the zenith's blue but does not yield the solar-sky purple light [10]. However, including a realistic vertical distribution of dust makes the zenith bluer and forms a purple light, with the former attributed to dust preferentially extinguishing longer wavelengths in direct sunlight. One of their fundamental conclusions is that "the increased blueness of the zenith sky during twilight can be explained without invoking the presence of atmospher[ic] dust, but does require the presence of ozone."

In 1974, Blättner *et al.* [11] used Monte Carlo techniques to simulate multiple scattering during twilight in purely molecular atmospheres, some of which include ozone. Although they rely on color ratios rather than colorimetry to assess ozone's visible effects, their model's skylight spectra show that adding a realistic ozone distribution makes its sky bluer during twilight. They concur with Dave and Mateer that the purple light cannot be generated by an exclusively molecular atmosphere. Adams *et al.* [12] drew similar conclusions from their colorimetric simulations of single-scattering atmospheres: without ozone, the twilight zenith is yellowish or nearly achromatic, but with ozone, the entire circumzenithal sky is some variety of blue. Like Dave and Mateer they calculate that, compared with an aerosol-free atmosphere, normal aerosol levels increase the purity of blue skylight at the zenith. They claim that this occurs because of the "greater increase in absorption at red than at blue wavelengths for the [direct] solar radiation up to the scattering point." In fact, trebling aerosol content in their model further reddens the circumsolar sky and makes the zenith bluer still. A few years later, Coulson analyzed twilight measurements of zenith skylight taken atop Mauna Loa, Hawaii [13]. In discussing twilight's temporal trends in relative intensity and color ratio, Coulson notes that both are clearly marked by ozone's absorption maximum near 600 nm.

2. Photographing Antarctic Twilights: A Sky-Color–Ozone Correlation?

Textbooks, articles, and popular-level books all now routinely describe ozone's central role in creating blue zeniths during twilight [14–19]. One of us (Hoeppe) has added a book to this growing list [20], in which he wonders whether Antarctica's especially large seasonal changes in column total ozone [21] might *visibly* affect twilight colors there. After all, Hulburt explicitly makes this connection: "But near sunset and throughout twilight ozone affects the sky color profoundly. For example, in the absence of ozone the zenith sky would be a grayish green-blue at sunset becoming yellowish in twilight, but with ozone the zenith sky is blue at sunset and throughout twilight (as is observed) …" [22]. Hoeppe recognized that a unique test of this connection might be made in Antarctica, and so set about establishing the funding and collaborations needed to make such a test possible.

At the outset we assumed that, all other things being equal, larger ozone concentrations will yield bluer clear twilights at the same unrefracted sun elevation h_0. This assumption stems from the extensive literature cited above, which features ozone-absorption models ranging in complexity from simple single scattering to multilayer multiple scattering. To illustrate these two extremes, Fig. 1 plots zenith chromaticities as predicted by the Bohren and Clothiaux model [23] and by LOWTRAN7 [24]. Figure 1 is a close-up view of the CIE 1976 uniform-chromaticity-scale (UCS) diagram, and it includes such colorimetric landmarks as part of the Planckian locus and its corresponding color-temperature limits. The older LOWTRAN7 is used here because the newer MODTRAN4 and MODTRAN5 calculate multiple-scattering contributions to daylight and skylight by assuming a plane-parallel atmosphere. In our MODTRAN version (version 4.3), this has the side effect of producing nonphysical spectra in the visible for $h_0 \le 0°$.

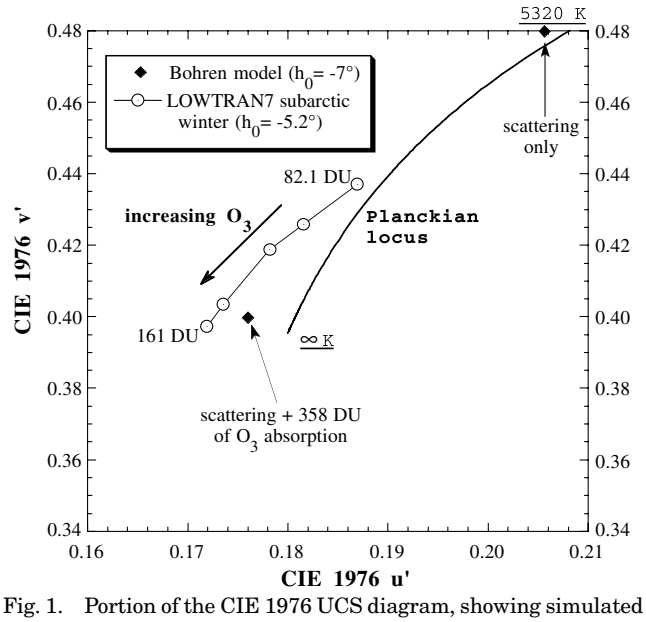

Fig. 1. Portion of the CIE 1976 UCS diagram, showing simulated zenith chromaticity coordinates u', v' for different unrefracted sun elevations h_0 during twilight and for different amounts of ozone (O_3). The Bohren and Clothiaux model uses molecular single scattering either without ozone or with absorption by 358 column total Dobson units (DU) of ozone. The chromaticity curve generated by LOWTRAN7's subarctic winter model is drawn in order of increasing ozone concentration.

In Fig. 1, the Bohren model's two chromaticities are calculated using single scattering of transmitted sunlight, either with or without ozone absorption along its path to the zenith. Adding a realistic 358 Dobson units (DU) of ozone [25] makes the zenith sky much bluer, although we later consider an important perceptual caveat to this conclusion. Similarly, LOWTRAN7 chromaticities [26] in Fig. 1 arc toward higher correlated color temperatures (CCTs) as ozone amounts increase. Each model's chromaticities in fact extend beyond infinite CCT, the purest blue that can be produced by molecular scattering alone [27]. These colorimetric results support the consensus view that, all other parameters held constant, increasing ozone concentrations consistently increase zenith blueness during civil twilight (*i.e.*, the period when $0° \geq h_0 \geq -6°$).

Does this correlation exist in nature? To answer this seemingly simple question, we start by describing our experimental tools and techniques in some detail. First, photographic calibration techniques developed earlier [28] are used to extract accurate colorimetric data from digital images. This in turn lets us measure daily changes in twilight colors at several fixed h_0. For our purposes, an ideal Antarctic site for photographing twilight colors has both a year-round research staff and a suite of instruments for acquiring meteorological data during photography. Facilities at Neumayer Station in Queen Maud Land (70° 40′ S, 8° 16′ W, 43 m above mean sea level) meet these two requirements well. Neumayer is operated by the Alfred Wegener Institute for Polar and Marine Research (Bremerhaven, Germany), which has measured the station's vertical distribution of ozone with radiosondes several times per week since the early 1980s. Data from 1992–2009 show that column total ozone at Neumayer dips from an average of ~280 DU in December and July to ~130 DU in late September and October [29].

From January 2005–February 2006, one of us (Meyer) headed Neumayer Station. During his stay, he used a Nikon E5700 digital camera to take a series of photographs during clear evening twilights. These images were centered on (1) the zenith sky, (2) the solar or antisolar horizons [30], and (3) the sky 45° above the horizon; they were taken in 1° steps of h_0 from +1° to −5°. A leveled tripod was used to set the camera's elevation angle, and solar ephemeris calculations were used to schedule the photographs and to help aim the camera in azimuth after sunset. Although the camera determined exposure parameters automatically, its spectral response was held constant at one color temperature. We analyzed photographs taken during 13 twilights: two when column total ozone was near a maximum (March–May 2005), five during a transitional period (late August, early September, and late October), and six when ozone density was near its annual minimum (mid-September to mid-October). From this series, we used all 13 photographs of the antisolar sky taken at $h_0 \sim -4.1°$ and 10 images of the zenith sky at $h_0 \sim -5.2°$ (three twilights lack zenith images). We included the antisolar images because they sum the visible effects of atmospheric scattering and Chappuis-band ozone absorption over the longest possible optical paths. Although the zenith images have a slightly smaller color gamut [31], they are a useful standard of comparison with earlier work.

In Fig. 2, we plot the mean CIE 1976 u', v' chromaticities measured across each of our antisolar and zenith images. Every plotted chromaticity coordinate is the average for one day (and one image) at the specified h_0, with all chromaticities averaged over skylight fields of view (FOVs) that span ~52° × 39° for the zenith images and ~52° × 32° for the antisolar images. The antisolar FOVs are smaller because we exclude below-horizon pixels from our analyses; each mean chromaticity is calculated from at least 240,500 pixels. Figure 2 includes two useful color metrics: the MacAdam u' and v' just-noticeable differences (JNDs) [32] that are typical of its skylight colors. In principle, if any two chromaticities differ by more than 1 JND in u' or v', then most observers can distinguish the corresponding color pair. So if we could somehow simultaneously compare the different twilights' mean chromaticities, then Fig. 2 shows that we would discern differences among most of its zenith and antisolar colors.

Figure 2's most obvious feature is that zenith colors are distinctly bluer than their antisolar counterparts. The antisolar sky's illumination near sunset is dominated by reddened sunlight that is scattered in near-forward directions, and this reddening is due to spectrally selective extinction by molecules and

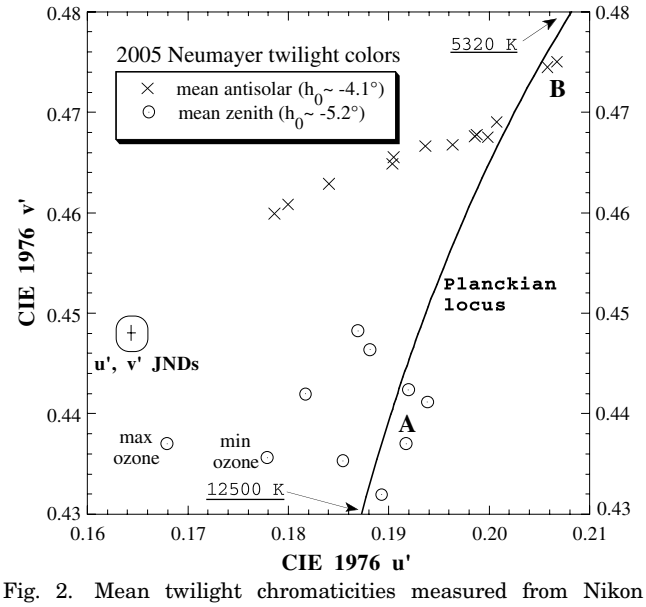

Fig. 2. Mean twilight chromaticities measured from Nikon E5700 digital images of the zenith sky (marked with circles) and antisolar sky (marked with ×s) at Neumayer Station, Antarctica from May–October 2005. Sun elevation h_0 is lower for the zenith images because these were taken ~15–20 min after the antisolar images during evening twilights. An asymmetric cross labeled "u', v' JNDs" indicates u' and v' MacAdam just-noticeable differences (JNDs) typical of this range of skylight chromaticities.

aerosols. Direct sunlight that is nearly as red illuminates part of the zenith path above us. Yet here the balance can shift from direct to diffuse illumination: redder direct sunlight that lights our zenith path is less intense precisely *because* additional extinction has removed more of its blue energy. As a result, the zenith path may be lit chiefly by bluish skylight scattered from many directions.

Now we can answer our question above about correlations between twilight colors and ozone. Certainly the complexity of models such as LOWTRAN7 suggests that no one atmospheric constituent by itself explains twilight's myriad colors. But historically, a strong case has been made that ozone absorption plus molecular scattering explains most of what we see during twilight, especially at the zenith. With that background in mind, examine Fig. 3. In it, we plot CCTs for Fig. 2's antisolar and zenith skylight chromaticities as functions of (nearly) concurrent measurements of column total ozone at Neumayer. Figure 3 also shows linear regression fits between ozone concentration and CCT for the two cases; using nonlinear fits would not change our qualitative conclusions. As expected, the correlation between zenith CCT and ozone is positive: more ozone makes the zenith sky bluer (*i.e.*, increases its CCT).

Yet the underlying statistics reveal that both correlations are quite weak. Given ozone concentrations in DU and CCTs in Kelvins, the linear zenith $\mathrm{CCT}(\mathrm{O_3}) = 9287.21 + 11.3099 * \mathrm{O_3}$. However, this fit's correlation coefficient r is only 0.3681, its t-statistic only 1.120, and the corresponding two-sided p-value is 0.2952. In other words, if we assume the statistical null hypothesis that *no* relationship exists between ozone and zenith CCT, then the probability of a t-statistic ≥ 1.120 occurring is almost 30% rather than some near-zero value [33]. So on purely statistical (rather than optical) grounds, we cannot reject the possibility that ozone concentrations are unrelated to zenith colors. Matters are even more tenuous for the antisolar CCTs, where the linear $\mathrm{CCT}(\mathrm{O_3}) = 9655.63 - 1.86848 * \mathrm{O_3}$, $r = -0.09196$, $t = -0.3063$, and the two-sided $p = 0.7651$. Thus the negative correlation between ozone and antisolar colors is nearly nil.

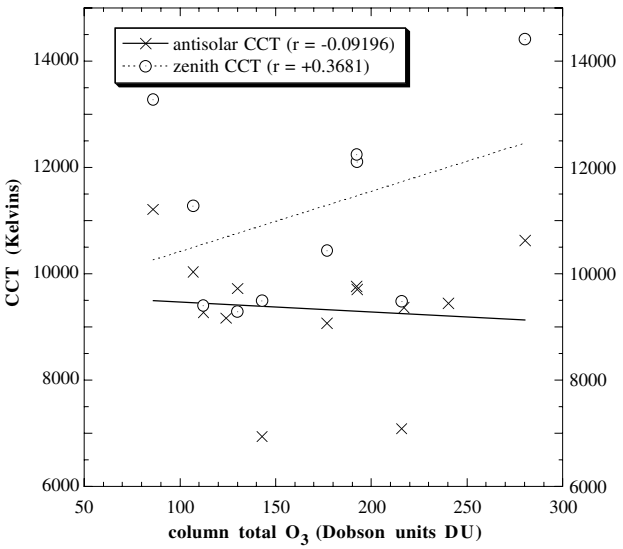

Fig. 3. Scatterplots of Fig. 2's antisolar and zenith skylight CCTs versus column total ozone as measured by radiosonde at Neumayer Station. For each sky direction, linear regression fits between ozone and CCT are statistically insignificant. Image sequences that are sorted in order of decreasing ozone concentration display these weak correlations for the (a) antisolar (Media 1) and (b) zenith skies (Media 2).

However convincing these statistics may be, they literally pale in comparison to viewing sequences of our Neumayer photographs (see Figs. 3(a) (Media 1) and 3(b) (Media 2); note date and DU labels at lower left). Each sequence is arranged in order of decreasing ozone concentration at the same h_0, yet neither sequence shows even a hint of color order. Especially striking are the first and last images in each sequence: these twilight skies are nearly the same blue, even though ozone concentrations are almost 200 DU lower in the last image (3 October 2005). Strong backscattering by aerosols in the antisolar sky often constitutes a larger *fraction* of its total signal than does aerosol scattering at the zenith. So we may be tempted to dismiss our antisolar results as somehow unrepresentative of the combined effects of molecular scattering and ozone absorption at the zenith. However, comparing the antisolar and zenith image sequences shows that redder antisolar colors are always paired with redder zenith colors on the same day. This makes sense, because reddened direct sunlight drives scattering everywhere in the unshaded twilight sky. Thus Fig. 3's negligible statistical correlation of antisolar colors with ozone does not render them optically meaningless in explaining the behavior of its zenith colors.

One sensible objection to Fig. 3's apparent color disorder is that we have not considered the vertical distribution of ozone. Figure 4 is a counterexample to this objection: zenith (and antisolar) sky colors differed visibly on these two days, even though their ozone soundings are not markedly different. The relative insensitivity of skylight colors to ozone distributions' vertical details is not surprising. For example, even the radical simplification of converting a realistic nonuniform ozone profile to a uniform layer at 20–35 km changes the zenith's skylight spectrum only minimally [34]. Furthermore, Fig. 4's column total ozone offers no help with this puzzle, since it is slightly less on the day with a bluer twilight sky (12 October 2005).

What can explain the discrepancy between longstanding theories about ozone's effects on twilight colors and their actual appearance in our measurements? Part of the answer comes from considering the role of aerosols. Adams *et al.* did so several decades ago [35], but the problem is well worth reexamining. Neumayer Station's aerosol ions are dominated by sea salt, methane sulfonic acid, and non-sea-salt sulfate [36], with the dispersed phase

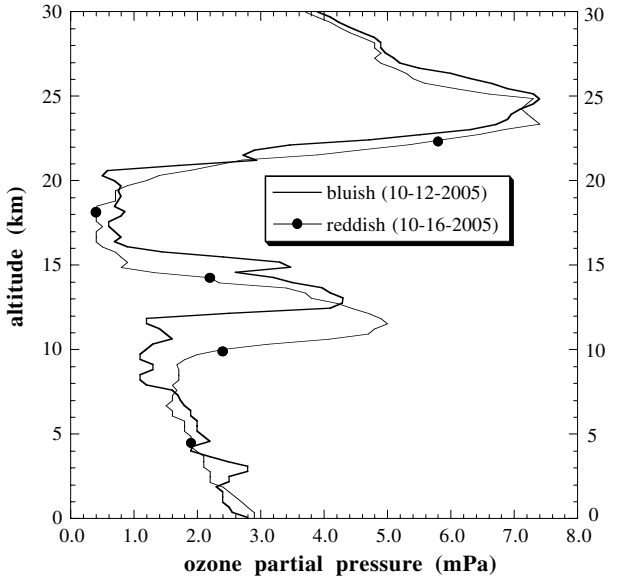

Fig. 4. Similar radiosonde profiles of ozone partial pressures at Neumayer Station during twilights that were either visibly bluish (12 October 2005, $O_3 = 106.9$ DU, mean CCT ~ 10030 K) or reddish (16 October 2005, $O_3 = 112.3$ DU, mean CCT ~ 9270 K) at the zenith when $h_0 \sim -5.2°$. See Figs. 3(a) (Media 1) and 3(b) (Media 2) to compare photographs of these two twilights.

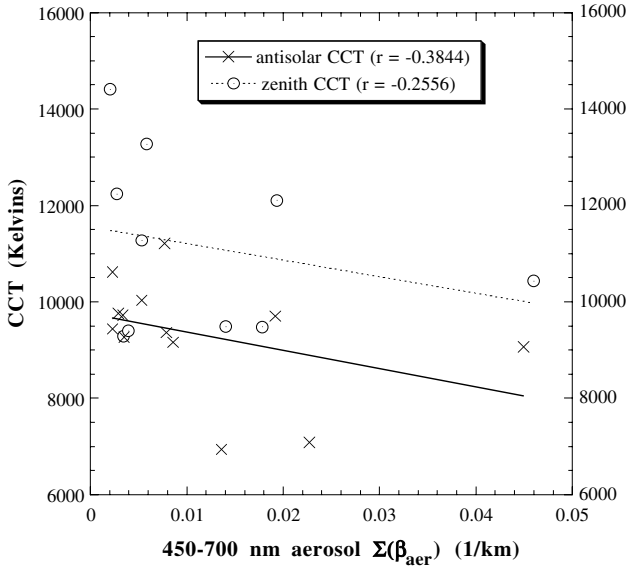

Fig. 5. Scatterplots of Fig. 2's antisolar and zenith skylight CCTs versus combined surface aerosol extinction coefficients $\Sigma(\beta_{aer})$ as measured by nephelometer at Neumayer Station. Linear regression fits between $\Sigma(\beta_{aer})$ and CCT are statistically insignificant: null-hypothesis two-sided p-values are 0.1947 and 0.4760 for the antisolar and zenith data, respectively.

consisting chiefly of very small ice particles whose size distribution is approximately bimodal lognormal (broad peaks occur near 100 and 500–900 nm) [37]. Several times per hour, the Air Chemistry Laboratory at Neumayer measures and archives surface-based aerosol optical properties that include total extinction coefficients $\beta_{aer}(\lambda)$ at wavelengths λ of 450, 550, and 700 nm [38].

In Fig. 5, we plot Fig. 3's antisolar and zenith CCTs as functions of the combined β_{aer} at these wavelengths (call this sum $\Sigma(\beta_{aer})$). During civil twilight, direct sunlight follows quasi-horizontal paths whose mean aerosol optical thickness $\tau_{aer} \propto \Sigma(\beta_{aer})$ at the surface (note that τ_{aer} is a path-integrated quantity, whereas β_{aer} is not). Although Fig. 5's linear correlations between surface visible-λ β_{aer} (and thus τ_{aer}) and CCT are scarcely larger than those for ozone, for us their optical significance is that both the antisolar and zenith fits are negative. Based on their null-hypothesis p-values, Fig. 5's fits show that aerosol optical thickness is at least as significant in (partially) explaining twilight colors as ozone concentration is.

As surface τ_{aer} increases and meteorological range V' decreases (because $V' \propto 1/\beta_{aer}$), the Neumayer data indicate that directly transmitted sunlight tends to become redder (*i.e.*, its CCT decreases). In turn, this redder direct-beam illumination makes scattered skylight redder. Figure 3(a) (Media 1) provides visual evidence for this in its frames date-stamped 8, 11, and 16 September 2005 [39]: surface features are distinctly reddened on these days, which have three of the four highest $\Sigma(\beta_{aer})$ values. Visually, the net result of this reddening is to make the sky slightly *purplish* during twilight, especially at the zenith where skylight is consistently bluer. Colorimetrically, this reddening manifests itself in our measured chromaticities as a shift to the right of the Planckian locus. Two such shifts define Fig. 2's chromaticity clusters **A** and **B**, and these clusters occurred on the four days with the largest $\Sigma(\beta_{aer})$ at Neumayer.

Similar results follow from LOWTRAN7 simulations. If direct sunlight is reddened enough by aerosol extinction, this can sometimes outweigh the bluing caused by ozone absorption. For example, in Fig. 6 we draw two LOWTRAN7 chromaticity curves for zenith skylight as a function of meteorological range V' in two otherwise identical atmospheres with different ozone amounts. At a constant $h_0 = -5.2°$, the model predicts a very clear atmosphere's zenith can be bluer (case **C**) than one in a more turbid atmosphere (case **D**), even though case **C** has less ozone. However, this explanation only goes so far in LOWTRAN7, because reducing ozone still further eventually eliminates any overlap between the two chromaticity curves. Interestingly, increasing turbidity does not make the zenith redder without limit: for $V' < 1.3$ km, direct sunlight is attenuated so much along paths near the surface that this ever-more reddened light contributes less and less to scattered zenith radiances. In Fig. 6, the colorimetric signature of these diminishing contributions from highly attenuated sunlight is the reversal in each chromaticity curve near its low-V' end (note the small chromaticity "hooks" there).

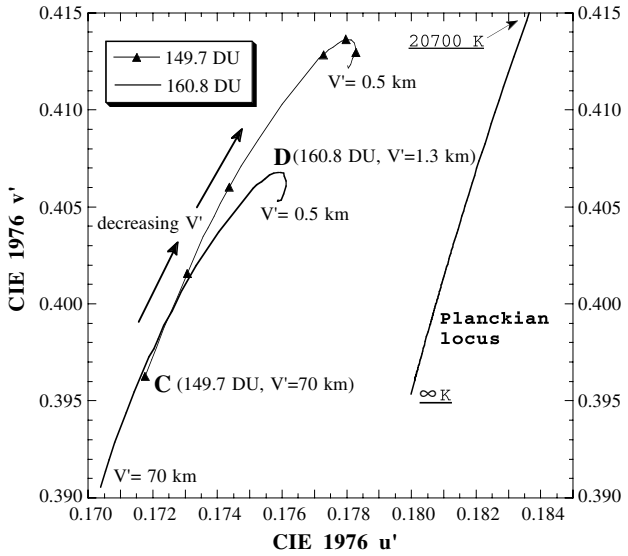

Fig. 6. LOWTRAN7 zenith chromaticities as functions of meteorological range V' for two different ozone concentrations (subarctic winter model, $h_0 = -5.2°$, $V' = 0.5$–70 km). In this comparison, a very clear atmosphere with less ozone (case **C**) can have a bluer zenith than a more turbid atmosphere with more ozone (case **D**).

3. Ozone, Aerosols, and Zenith Twilight Colors at a Midlatitude Site

Perhaps our choice of measuring site has obscured ozone's contributions to twilight colors. To avoid this possible pitfall, in Fig. 7 we plot twilight chromaticities found far from Antarctica's pristine atmosphere. We measured Fig. 7's zenith colors at the midlatitude site of Owings, Maryland (38° 41′ N, 76° 35′ W, elevation = 12 m) during 20 clear twilights in 2000, 2001, and 2010 when $h_0 \sim -5.2°$. Unlike Fig. 2's chromaticities, those in Fig. 7 are calculated from radiance spectra acquired with a Photo Research PR-650 spectroradiometer [40]. One obvious difference between the two figures is that Fig. 7's colors are much bluer, with nearly all of them lying beyond infinite CCT. Some of this colorimetric difference stems from FOV differences between the camera and radiometer: Fig. 2's camera-derived chromaticities are averaged across a much larger solid angle of circumzenithal sky, and so include greater departures from zenith skylight. Yet colorimetric differences persist in zenith colors even if we match the radiometer's FOV when calculating camera averages.

Much as Figs. 3 and 5 do, Fig. 8 shows correlations between Fig. 7's zenith colors and either ozone concentration or aerosol extinction. However, Fig. 7's chromaticities require a different color metric than CCT in order to construct such a scatterplot. We first determine a "color center" in Fig. 7 (see × near its right side) from which we calculate colorimetric dominant wavelengths λ_d. Although this color center's exact position is not crucial, we place it so that if Fig. 7 were isotropically scaled, then its colorimetric extremes **E** and **F** would (1) be equidistant from the color center and (2) subtend a central angle of 90° at it. A straight line segment that connects the color center, a skylight chromaticity, and the spectrum locus then yields a one-dimensional color measure that is geometrically, if not perceptually, equivalent to λ_d measured from a true achromatic point. These λ_d equivalents are Fig. 8's ordinate values.

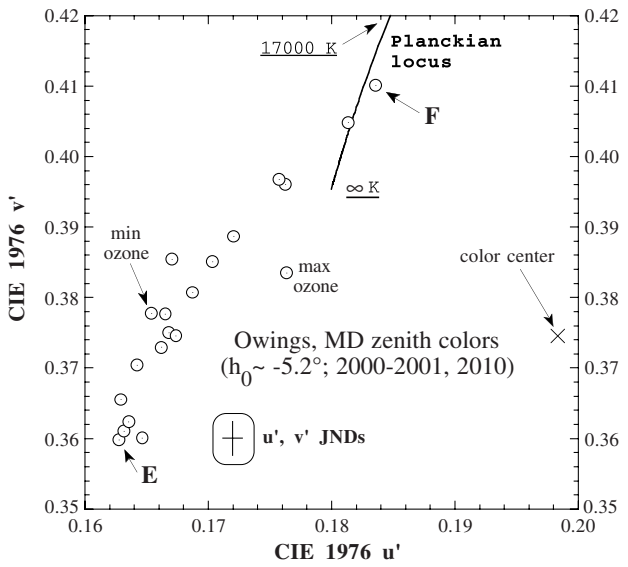

Fig. 7. Zenith chromaticities measured during 20 clear twilights at Owings, Maryland with a Photo Research PR-650 spectroradiometer (1° field of view). The underlying skylight radiance spectra were measured during January–February 2000, January 2001, and April–May 2010 for $-5.22° \le h_0 \le -5.13°$. Chromaticities **E** and **F** are this figure's colorimetric and spectral extremes.

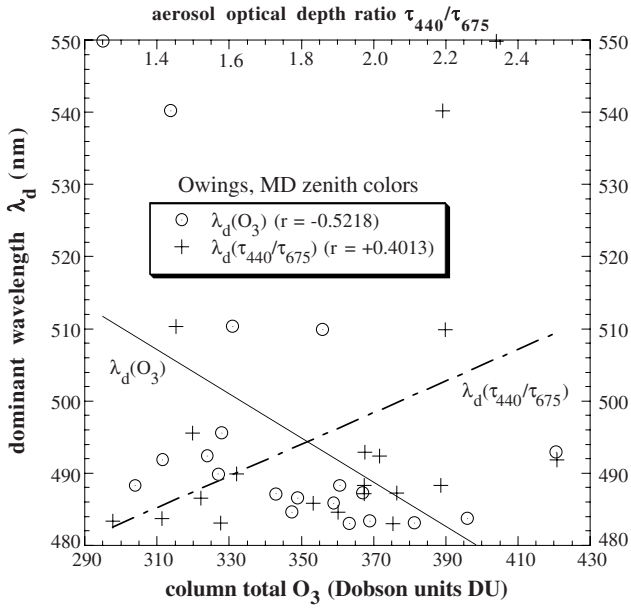

Fig. 8. Scatterplots of zenith skylight λ_d at Owings, Maryland versus (1) column total ozone and (2) ratio of normal aerosol extinction at 440 and 675 nm, $\tau_{\mathrm{aer},440}/\tau_{\mathrm{aer},675}$. The linear correlation $r = -0.5218$ between λ_d and ozone is statistically significant at the 2% level (two-sided p-value = 0.0183), whereas the aerosol $r = +0.4013$ is significant at the 10% level ($p = 0.0795$). Because λ_d increases as CCT decreases, r's signs here are reversed compared with zenith r values in Figs. 3 and 5.

Figure 8 has two different abscissa scales: its top scale is calculated from normal aerosol optical depth $\tau_{\mathrm{aer},\lambda}$ for extinction as measured by sun photometers [41] and its bottom scale is column total ozone concentration as measured by Dobson spectrophotometers [42]. The top scale in Fig. 8 is the ratio of τ_{aer} at $\lambda = 440\,\mathrm{nm}$ and 675 nm, which is similar to the Angström coefficient and so gives a measure of aerosol extinction's spectral dependence. The smallest aerosol particles extinguish shorter-λ light more efficiently than longer-λ light, and this efficiency grows as the ratio $\tau_{\mathrm{aer},440}/\tau_{\mathrm{aer},675}$ increases. As a result, transmitted sunlight is redder for larger $\tau_{\mathrm{aer},440}/\tau_{\mathrm{aer},675}$ values, provided that either optical thickness is large enough to perceptibly alter this light [43].

At first glance, linear correlation coefficients between zenith λ_d and either ozone or aerosols ($r = -0.5218$ and $r = +0.4013$, respectively) may not *seem* much greater than comparable pairings in Figs. 3 and 5. Yet their null-hypothesis p-values tell a very different story: both indicate statistically significant (albeit weak) relationships among the parameters, with $p = 0.0183$ for $\lambda_d(\mathrm{O_3})$ and $p = 0.0795$ for $\lambda_d(\tau_{\mathrm{aer},440}/\tau_{\mathrm{aer},675})$. Even eliminating Fig. 8's statistical outliers at $\lambda_d > 540\,\mathrm{nm}$ does not materially change the quality of these correlations. Yet as useful as it is, Fig. 8 can provide no insights about why the correlations themselves are not larger.

For that insight, we turn to the relative radiance spectra of Fig. 9. Colorimetric extremes **E** and **F** in Fig. 7 (whose dates are 17 January 2000 and 7 January 2000, respectively) are also its spectral extremes in the sense that their underlying radiance spectra are its least congruent. To see how much zenith skylight changes spectrally between late afternoon and twilight on these two dates, we calculate ratios $L_{\mathrm{rel},\lambda} = L_\lambda(h_0 = -5.2°)/L_\lambda(h_0 = +4.5°)$ and plot the resulting spectra in Fig. 9. Its $L_{\mathrm{rel},\lambda}$ spectra show how the greatly increased ozone absorption and aerosol extinction during twilight *combine* to change the color of scattered sunlight reaching us at the surface, where zenith radiances have decreased more than 100-fold.

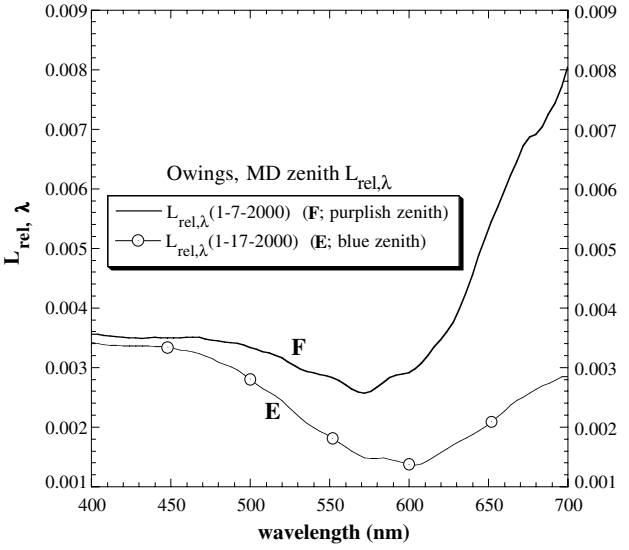

Fig. 9. Relative spectral radiances $L_{\mathrm{rel},\lambda}$ measured at $h_0 \sim -5.2°$ on two days with visibly different zenith colors at Owings, Maryland. The ratio $L_{\mathrm{rel},\lambda} = L_\lambda(h_0 = -5.2°)/L_\lambda(h_0 = +4.5°)$ shows the spectral shifts that skylight undergoes between late afternoon and late civil twilight on these dates.

Figure 9's most prominent features are its broad $L_{\mathrm{rel},\lambda}$ minima near 575–600 nm. These clearly are the result of ozone absorption [44], with spectrum **F**'s minimum effectively shifted to shorter wavelengths by the steep rise in $L_{\mathrm{rel},\lambda}$ beyond 600 nm. This spectral rise is likely caused by changes in aerosol extinction: not only is the total visible-λ τ_{aer} nearly 50% larger on 7 January 2000, but so is the $\tau_{\mathrm{aer},440}/\tau_{\mathrm{aer},675}$ ratio. As a consequence, direct sunlight is distinctly reddened on 7 January 2000, and field notes for that day record not only a vivid purple light in the solar sky, but also a distinctly lavender or purplish zenith when $h_0 \sim -3°$. Conversely, the purple light was nearly absent on 17 January 2000 and the zenith did not look at all purplish. The two dates also have distinctly different ozone concentrations, with 295 DU on 7 January 2000 (spectrum **F**) and ~381 DU on 17 January 2000 (spectrum **E**).

Thus spectrum **F** is a case where both atmospheric constituents work in concert to make zenith skylight redder and less blue: longer wavelengths in direct sunlight undergo less extinction by ozone *and* by aerosols. Naturally these processes need not be coordinated, and that explains optically the relatively low statistical correlations between sky color and either constituent in Figs. 3, 5, and 8. As another example, consider cases in Figs. 2 and 7 where the dynamic range of ozone concentration is much larger at Neumayer (3.26∶1) than at Owings (1.38∶1). In each figure, zenith chromaticities of these dynamic-range pairs are labeled as "min ozone" and "max ozone" (measured aerosols did not change markedly at either site). Despite the smaller ozone dynamic range at Owings, not only is its chromaticity pair much farther apart, but zenith color is actually nominally bluer for minimum ozone (see Fig. 7). In addition, our past research on the purple light reveals yet another mechanism for creating some distinctly blue twilights: shadows cast by distant clouds below the observer's sunset or sunrise horizon [45]. Simply preventing reddened direct sunlight from illuminating the atmosphere above us is by itself enough to make the sky blue during much of civil twilight. This too will decrease the correlation between ozone concentration and blues of the twilight sky. A more complete analysis naturally would include the *areal* distributions of ozone and aerosols, but data with sufficiently high resolution in both time and all three spatial dimensions does not seem to exist for either of our sites.

4. Ozone Blues: Optics, Experience, and Visual Perception during Twilight

Why then does ozone absorption figure so prominently in popular and scientific writing on twilight colors? First, ozone content really *can* visibly affect zenith blueness during twilight. But so too can extinction by tropospheric aerosols and even shading by clouds, as shown above. Thus one can tacitly overemphasize ozone's role simply by not dwelling on those of aerosols and clouds. Hulburt himself is quite circumspect about his discovery, saying only that ozone made his model zenith twilight sky "blue or blue-purple, perhaps somewhat unsaturated." Nor does he neglect the troposphere's role, noting that "there is probably always some atmospheric dust or haze present which may either increase or decrease [spectral brightness] B depending on its distribution" [46]. Adams *et al.* and Dave and Mateer also assess the colorimetric effects of absorption and scattering by dust and aerosols, but they make the odd claim that these scatterers preferentially absorb *longer* visible wavelengths. This would make transmitted sunlight bluer, not redder. Although blue suns and moons can occur [47,48], they are rarities far removed from our daily experience of atmospheric aerosols that redden transmitted sunlight.

Second, as is so often true in life, location matters. Hulburt's colleagues, Coulson, and we ourselves [49] have measured or admired twilight zeniths from mountaintop locations that are above most or all of the planetary boundary layer. At these altitudes (*e.g.*, Hulburt's data was collected from altitudes of 2.5–2.8 km), tropospheric aerosols may well be of little importance in determining the spectrum of zenith skylight. But near the bottom of the troposphere, its single- and multiple-scattering contributions to the sunlit and shaded atmosphere above us often outweigh changes in stratospheric absorption and scattering.

So where you measure determines what you see and what you consider important. For example, consider Fig. 10's LOWTRAN7 chromaticity curve of zenith color as a function of observer altitude z above the Earth's surface. The same subarctic winter model is used as before, but now with $V' = 1.0$ km. When $h_0 = -5.2°$ at the surface ($z = 0$ km), the lowest parts of our viewing path toward the zenith are in shadow. Much of the signal we receive then is bluish skylight that has been multiply scattered within the surface layer above us where aerosol number densities are largest. As we rise through this shallow layer in Fig. 10, two trends coexist: (1) zenith skylight gets brighter because fewer downward-moving photons are extinguished, and so (2) reddened sunlight transmitted in near-forward directions begins to dominate scattered photons that reach us. Thus the zenith becomes brighter and redder until $z \sim 0.6$ km, at which altitude (3) transmitted sunlight passing above us has undergone relatively little reddening and (4) we receive progressively bluer skylight that is less and less affected by the rapidly decreasing aerosol

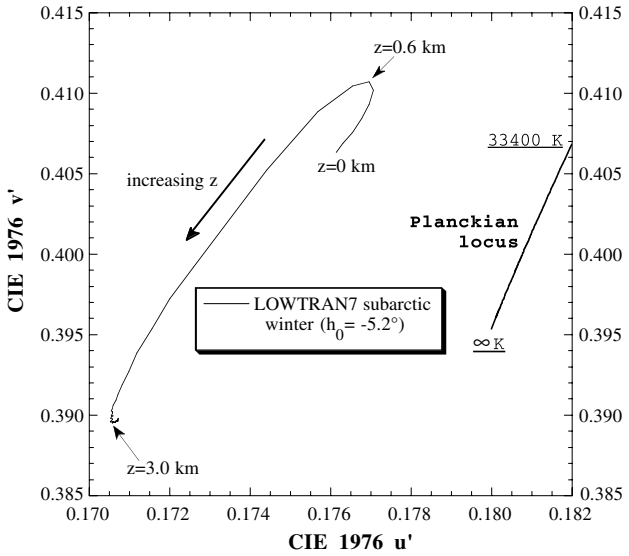

Fig. 10. LOWTRAN7 zenith chromaticities as a function of observer altitude z above the surface (subarctic winter model, $h_0 = -5.2°$, $z = 0$–5 km, $V' = 1.0$ km). Below $z = 0.6$ km, increasing z makes zenith skylight redder as the observer rises through the densest part of the surface aerosol layer and so receives less multiply scattered skylight. At higher z, rapidly diminishing aerosol extinction above the observer makes skylight bluer.

concentrations above us. The net result is that from $z = 3$–5 km (our simulation's upper bound) in Fig. 10, skylight scarcely changes color. If you view and measure zenith skylight from such altitudes, then visual experience and measurements both indicate that ozone matters much more than aerosols in determining the color of zenith skylight.

Finally, we must acknowledge an important perceptual caveat. Everything said so far assumes that you can in fact *perceive* colors wherever and whenever you look in the clear sky during civil twilight. Sadly, this is not so. In our experience, seeing any color at the zenith becomes problematic at $h_0 \sim -4.5°$ when zenith luminances typically are 1–2 cd/m^2. Such luminance levels are less than the bright limit of mesopic vision [50], and so our visual systems have difficulty in producing color sensation from skylight this dark (color vision is still possible in the brighter solar sky). Thus no matter how artful our radiative transfer arguments are about skylight colors for $h_0 < -4.5°$, we (and others) are merely analyzing spectral and colorimetric details rather than describing direct visual experience. Regardless of how much aerosol extinction and ozone absorption shape skylight spectra then, we will never see twilight colors in this light.

5. Conclusions

Certainly the blues seen in clear twilight skies result primarily from ozone absorption rather than molecular scattering. Absorption in the stratosphere by ozone's Chappuis bands is most visible during twilight because direct sunlight's optical paths through the atmosphere are largest then. Work by Hulburt and others has painstakingly established these basic

facts, which our measurements and modeling above reconfirm (Figs. 1, 2, 7, and 9). However, our research also shows that neither column total ozone nor its vertical distribution (Fig. 4) can explain the full range of observed twilight colors, including at the zenith. This is clear from the weak statistical correlations that we measured between ozone concentrations and sky colors at Neumayer Station, Antarctica and at Owings, Maryland (Figs. 3, 5, and 8). Even though Neumayer and much of Antarctica experience large ozone depletions during the austral spring, these alone are insufficient to account consistently for the colors of clear twilights seen from low altitudes.

For realistic simulations of these colors, at a minimum we must also consider spectral extinction by aerosols. Even so pristine an environment as Neumayer's can have large daily fluctuations in its aerosol composition and concentrations. Larger aerosol concentrations tend to redden the sunlight that illuminates atmospheric paths, whereas increased ozone amounts make both it and scattered skylight bluer. These atmospheric constituents vary independently of one another, and the resulting spectral changes to skylight may work in the same or opposite color directions (see Figs. 7 and 9). As in the related phenomenon of the purple light, optical conditions in the troposphere (*e.g.*, haze or cloud shadows) are vitally important, and these can undergo large daily and even hourly changes. Thus the troposphere and stratosphere acting together determine sky colors seen during civil twilight.

Lee was generously supported by United States National Science Foundation (NSF) grant AGS-0914535 and by the United States Naval Academy's Departments of Oceanography and Physics. Opinions, findings, and conclusions or recommendations expressed in this paper are those of the authors and do not necessarily reflect the views of the National Science Foundation. We thank the Alfred Wegener Institute for Polar and Marine Research and the scientists and technicians at Georg von Neumayer Station for their able logistical support of Meyer's 2005 photographic campaign. The Alfred Wegener Institute is funded by the German Federal Ministry for Education and Research (BMFT). We also thank Oliver Montenbruck of the Deutsches Zentrum für Luft- und Raumfahrt (Oberpfaffenhofen, Germany) for computing vital solar ephemeris data used at Neumayer. Photographic equipment was kindly funded by the Verlag Spektrum der Wissenschaft (Heidelberg, Germany).

References and Notes

1. E. O. Hulburt, "Explanation of the brightness and color of the sky, particularly the twilight sky," J. Opt. Soc. Am. **43**, 113–118 (1953).
2. J. Dubois, "Contribution a l'étude de l'ombre de la terre," Ann. Géophys. **7**, 103–107, 145–163 (1951).
3. M. Gadsden, "The colour of the zenith twilight sky: absorption due to ozone," J. Atmos. Terr. Phys. **10**, 176–180 (1957).
4. N. B. Divari, "Variations in the color of the twilight sky," Dokl. Akad. Nauk SSSR **122**, 795–798 (1958).
5. F. E. Volz and R. M. Goody, "The intensity of the twilight and upper atmospheric dust," J. Atmos. Sci. **19**, 385–406 (1962).
6. M. Gadsden, "The colour of the zenith twilight sky: absorption due to ozone," J. Atmos. Terr. Phys. **10**, 176–180 (1957).
7. G. V. Rozenberg, *Twilight: A Study in Atmospheric Optics* (Plenum, 1966), pp. 216, 236–249.
8. F. E. Volz, "Twilights and stratospheric dust before and after the Agung eruption," Appl. Opt. **8**, 2505–2517 (1969).
9. J. V. Dave and C. L. Mateer, "The effect of stratospheric dust on the color of the twilight sky," J. Geophys. Res. **73**, 6897–6913 (1968).
10. R. L. Lee, Jr. and J. Hernández-Andrés, "Measuring and modeling twilight's purple light," Appl. Opt. **42**, 445–457 (2003).
11. W. G. Blättner, H. G. Horak, D. G. Collins, and M. B. Wells, "Monte Carlo studies of the sky radiation at twilight," Appl. Opt. **13**, 534–547 (1974).
12. C. N. Adams, G. N. Plass, and G. W. Kattawar, "The influence of ozone and aerosols on the brightness and color of the twilight sky," J. Atmos. Sci. **31**, 1662–1674 (1974).
13. K. L. Coulson, "Characteristics of skylight at the zenith during twilight as indicators of atmospheric turbidity. 2: Intensity and color ratio," Appl. Opt. **20**, 1516–1524 (1981).
14. C. F. Bohren and E. E. Clothiaux, *Fundamentals of Atmospheric Radiation* (Wiley-VCH, 2006), pp. 409–415.
15. C. F. Bohren and A. B. Fraser, "Colors of the sky," Phys. Teach. **23**, 267–272 (1985).
16. S. D. Gedzelman, "Simulating colors of clear and partly cloudy skies," Appl. Opt. **44**, 5723–5736 (2005).
17. D. K. Lynch and W. Livingston, *Color and Light in Nature* (Cambridge, 1995), p. 38.
18. J. C. Naylor, *Out of the Blue: A 24-hour Skywatcher's Guide* (Cambridge, 2002), p. 71.
19. P. Pesic, *Sky in a Bottle* (MIT Press, 2005), pp. 173–175.
20. G. Hoeppe, *Why the Sky is Blue: Discovering the Color of Life* (Princeton, 2007), pp. 259–260, 308 n. 16.
21. J. C. Farman, B. G. Gardiner, and J. D. Shanklin, "Large losses of total ozone in Antarctica reveal seasonal ClO_x/NO_x interaction," Nature **315**, 207–210 (1985). For our purposes, the atmospheric chemistry and dynamics that drive Antarctica's ozone fluctuations are just means to an optical end, so we do not consider its ozone meteorology in detail.
22. E. O. Hulburt, "Explanation of the brightness and color of the sky, particularly the twilight sky," J. Opt. Soc. Am. **43**, 113–118 (1953).
23. C. F. Bohren and E. E. Clothiaux, *Fundamentals of Atmospheric Radiation* (Wiley-VCH, 2006), pp. 409–415.
24. The LOWTRAN7 radiative transfer model is described in R. W. Fenn, S. A. Clough, W. O. Gallery, R. E. Good, F. X. Kneizys, J. D. Mill, L. S. Rothman, E. P. Shettle, and F. E. Volz, "Optical and infrared properties of the atmosphere," *Handbook of Geophysics and the Space Environment*, A. S. Jursa, ed. (Air Force Geophysics Laboratory, Hanscom Air Force Base, 1985), pp. 18:44–51.
25. A Dobson unit or DU is 2.69×10^{20} O_3 molecules/m^2, equivalent to 100 times the thickness in millimeters of total column ozone reduced to a uniform layer at surface pressure and 0 °C.
26. LOWTRAN7 model parameters used throughout this paper include a default subarctic winter atmospheric profile of temperature, pressure, humidity, and gas mixing ratios; a surface temperature of −10 °C; tropospheric aerosols typical of rural sites; background stratospheric dust and other aerosols (*i.e.*, ordinary rather than volcanic twilights); no clouds or rain; multiple scattering; a surface diffuse albedo of 0.85 that simulates snowcover; and Mie aerosol phase functions. To decrease ozone concentration from its maximum in the subarctic

winter model, we use different vertical distributions of ozone from other LOWTRAN7 default models.
27. C. F. Bohren and A. B. Fraser, "Colors of the sky," Phys. Teach. **23**, 267–272 (1985).
28. R. L. Lee, Jr., "Measuring overcast colors with all-sky imaging," Appl. Opt. **47**, H106–H115 (2008).
29. Neumayer Station meteorological data is archived at http://www.awi.de/en/infrastructure/stations/neumayer_station/observatories/meteorological_observatory/data_access/.
30. Images that include the topographic horizon are centered a few degrees above it.
31. See R. L. Lee, Jr., "What are 'all the colors of the rainbow'?," Appl. Opt. **30**, 3401–3407, 3545 (1991) for a quantitative definition of chromaticity gamut.
32. MacAdam JNDs are described in G. Wyszecki and W. S. Stiles, *Color Science: Concepts and Methods, Quantitative Data and Formulae* (Wiley, 1982, 2nd ed.), pp. 306–310.
33. Smaller p-values mean that the observed correlation is *less* likely to have arisen by chance. Thus for a given r, a smaller p-value indicates higher confidence in r's reliability.
34. C. F. Bohren and E. E. Clothiaux, *Fundamentals of Atmospheric Radiation* (Wiley-VCH, 2006), Fig. 8.15.
35. C. N. Adams, G. N. Plass, and G. W. Kattawar, "The influence of ozone and aerosols on the brightness and color of the twilight sky," J. Atmos. Sci. **31**, 1662–1674 (1974).
36. R. Weller and A. Lampert, "Optical properties and sulfate scattering efficiency of boundary layer aerosol at coastal Neumayer Station, Antarctica," J. Geophys. Res. **113**, D16208 (2008).
37. C. Rathke, J. Notholt, J. Fischer, and A. Herber, "Properties of coastal Antarctic aerosol from combined FTIR spectrometer and sun photometer measurements," Geophys. Res. Lett. **29**, 2131 (2002).
38. Neumayer Station aerosol data is archived at http://www.awi.de/en/infrastructure/stations/neumayer_station/observatories/air_chemistry_observatory/data_download/.
39. All date stamps in Fig. 3(a) (Media 1) are for the ozone soundings closest in time to its photographs. These coincide with the photography and $\Sigma(\beta_{\mathrm{aer}})$ dates except for 11 September 2005, for which photographs were taken one day earlier.
40. PR-650 spectroradiometer from Photo Research, Inc., 9731 Topanga Canyon Place, Chatsworth, Calif. 91311. According to Photo Research, at specified radiance levels, a properly calibrated PR-650 measures luminance and radiance accurate to within $\pm 4\%$, has a spectral accuracy of ± 2 nm, and its CIE 1931 colorimetric errors are $x < 0.001$, $y < 0.001$ for a 2856 K blackbody (CIE standard illuminant A).
41. Sun photometer data on $\tau_{\mathrm{aer},\lambda}$ is acquired and archived by AERONET at http://aeronet.gsfc.nasa.gov. Figure 8's τ_{aer} data is from the stations closest to Owings: Goddard Space Flight Center in Greenbelt, Maryland and the Smithsonian Environmental Research Center in Edgewater, Maryland.
42. Surface-based Dobson spectrophotometer data is archived by the Meteorological Service of Canada at http://www.woudc.org/data_e.html. Figure 8's ozone data is from the stations closest to Owings: Wallops Island, Virginia and Goddard Space Flight Center in Greenbelt, Maryland.
43. Some aerosol concentrations and composition in this region are analyzed in B. I. Magi, P. V. Hobbs, T. W. Kirchstetter, T. Novakov, D. A. Hegg, S. Gao, J. Redemann, and B. Schmid, "Aerosol properties and chemical apportionment of aerosol optical depth at locations off the U. S. east coast in July and August 2001," J. Atmos. Sci. **62**, 919–933 (2005).
44. C. F. Bohren and E. E. Clothiaux, *Fundamentals of Atmospheric Radiation* (Wiley-VCH, 2006), Fig. 8.13.
45. R. L. Lee, Jr. and J. Hernández-Andrés, "Measuring and modeling twilight's purple light," Appl. Opt. **42**, 445–457 (2003).
46. E. O. Hulburt, "Explanation of the brightness and color of the sky, particularly the twilight sky," J. Opt. Soc. Am. **43**, 113–118 (1953).
47. C. F. Bohren, *Clouds in a Glass of Beer: Simple Experiments in Atmospheric Physics* (Wiley, 1987), pp. 91–97.
48. P. Pesic, "A simple explanation of blue suns and moons," Eur. J. Phys. **29**, N31–N36 (2008).
49. G. Hoeppe, *Why the Sky is Blue: Discovering the Color of Life* (Princeton, 2007), pp. 235–237.
50. G. Wyszecki and W. S. Stiles, *Color Science: Concepts and Methods, Quantitative Data and Formulae* (Wiley, 1982, 2nd ed.), p. 406.